Electronic Supplementary Material

Hidden phase uncovered by ultrafast carrier dynamics in thin Bi_2O_2Se

Hao Li,[a,b] *Adeela Nairan,*[c] *Xiaoran Niu,*[a,b] *Yuxiang Chen,*[d] *Huarui Sun,*[d] *Linqing Lai,*[e] *Jingkai Qin,*[e] *Leyang Dang,*[f] *Guigen Wang,*[f] *Usman Khan**[c] *and Feng He**[a,b]

a. State Key Laboratory on Tunable Laser Technology, Harbin Institute of Technology (Shenzhen), Shenzhen 518055, P. R. China

b. Guangdong Provincial Key Laboratory of Aerospace Communication and Networking Technology, Harbin Institute of Technology (Shenzhen), Shenzhen 518055, P. R. China. E-mail: hefeng2020@hit.edu.cn

c. Institute of Functional Porous Materials, School of Materials Science and Engineering, Zhejiang Sci-Tech University, Hangzhou 310018, P. R. China. E-mail: usmankhan.2017@tsinghua.org.cn

d. School of Science and Ministry of Industry and Information Technology, Key Laboratory of Micro-Nano Opto-electronic Information System, Harbin Institute of Technology (Shenzhen), Shenzhen, Guangdong 518055, P. R. China

e. Sauvage Laboratory for Smart Materials, School of Materials Science and Engineering, Harbin Institute of Technology (Shenzhen), Shenzhen 518055, P. R. China

f. Shenzhen Key Laboratory for Advanced Materials, School of Materials Science and Engineering, Harbin Institute of Technology (Shenzhen), Shenzhen 518055, P. R. China

S1. AFM images of Bi_2O_2Se thin films with different thicknesses.

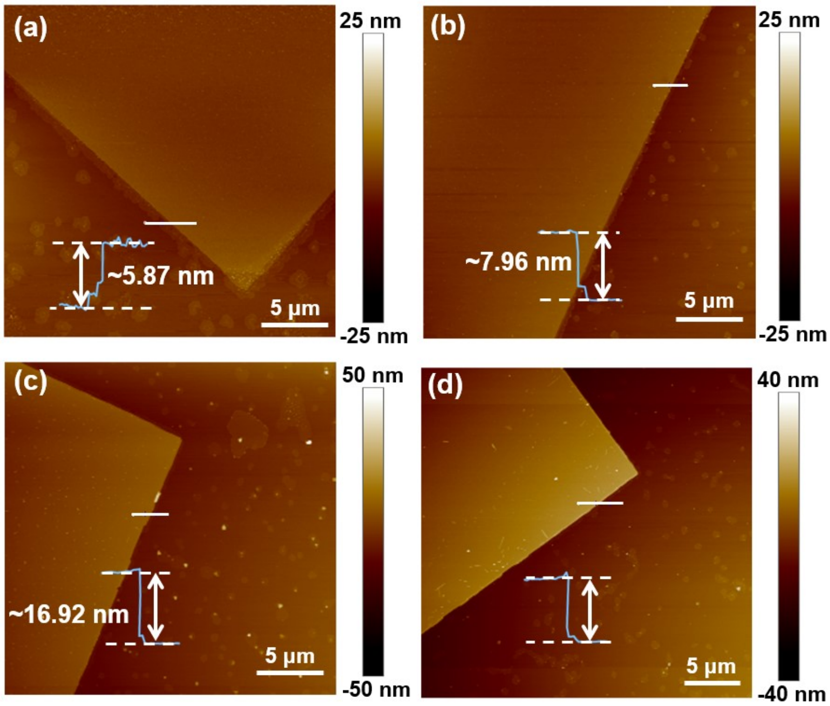

Figure S1. Additional AFM analysis of ultrathin Bi_2O_2Se films. AFM image of Bi_2O_2Se thin film with a thickness of (a) 5.87 nm, (b) 7.96 nm, (c) 16.92 nm, and (d) 22.44 nm.

S2. Transfer matrix method calculation

The transfer matrix method is commonly employed to determine the complex refractive index of materials.

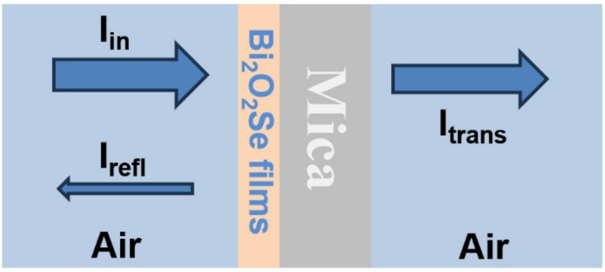

Figure S2. A diagram illustrating transfer matrix method.

Specifically, for the Air/Bi_2O_2Se and Bi_2O_2Se/Mica interfaces under consideration, the transfer matrices can be expressed as follows:

$$\mathrm{M}_{\text{interface}} = \frac{1}{t}\begin{pmatrix} 1 & r \\ r & 1 \end{pmatrix} \qquad \text{S1}$$

$$t = \frac{2\overline{n_1}}{\overline{n_1} + \overline{n_2}} \qquad \text{S2}$$

$$r = \frac{\overline{n_1} - \overline{n_2}}{\overline{n_1} + \overline{n_2}} \qquad \text{S3}$$

Where t and r are the transmission and the reflection of electric field, respectively.

Where $\overline{n_1}$ and $\overline{n_2}$ are the complex refractive index of the materials on the front and back sides of the interface. Since the thickness of mica is much thicker than the sample thickness, we consider it to be semi-infinite. The laser propagation inside the Bi_2O_2Se is modeled by a propagation matrix as:

$$\mathrm{M}_{\text{propagation}} = \begin{pmatrix} e^{-\frac{i2\pi \bar{n} d}{\lambda}} & 0 \\ 0 & e^{\frac{i2\pi \bar{n} d}{\lambda}} \end{pmatrix} \qquad \text{S4}$$

where $\bar{n}$ is the complex refractive index of Bi_2O_2Se, d is the thickness, and λ is the wavelength. So, the total transfer matrix can be written as:

$$\mathrm{M} = \mathrm{M}_{\text{Air/Bi}_2\text{O}_2\text{Se}} \times \mathrm{M}_{\text{propagation}} \times \mathrm{M}_{\text{Bi}_2\text{O}_2\text{Se/Mica}} = \begin{pmatrix} \mathrm{M}_{11} & \mathrm{M}_{12} \\ \mathrm{M}_{21} & \mathrm{M}_{22} \end{pmatrix} \qquad \text{S5}$$

The reflectance can be written as:

$$\mathrm{R} = \left| \frac{\mathrm{M}_{21}}{\mathrm{M}_{11}} \right|^2 \qquad \text{S6}$$

The transmittance can be written as:

$$T=\left|\frac{1}{M_{11}}\right|^2\times\frac{|n_{\mathrm{Mica}}|}{|n_{\mathrm{Air}}|} \quad \mathrm{S7}$$

With R and T from the experiment (Figure S2), the complex refractive index $\bar{n}=n+ik$ can be solved at each irradiance, where n and k are the real and imaginary part, respectively. Then, the absorption coefficient can be calculated as $\alpha=4\pi k/\lambda$. Results are summarized in Table S1.

Next, the initial carrier density N_0 is given by N_0 = (1-R-T)×F / ($d_{\mathrm{eff}}\times E_{\mathrm{ph}}$), where F represents the pump fluence, E_{ph} represents the photon energy. d_{eff} stands for the effective absorption depth, which is equal to the sample thickness since the laser penetration depth is much greater than the thickness of the sample.[1]

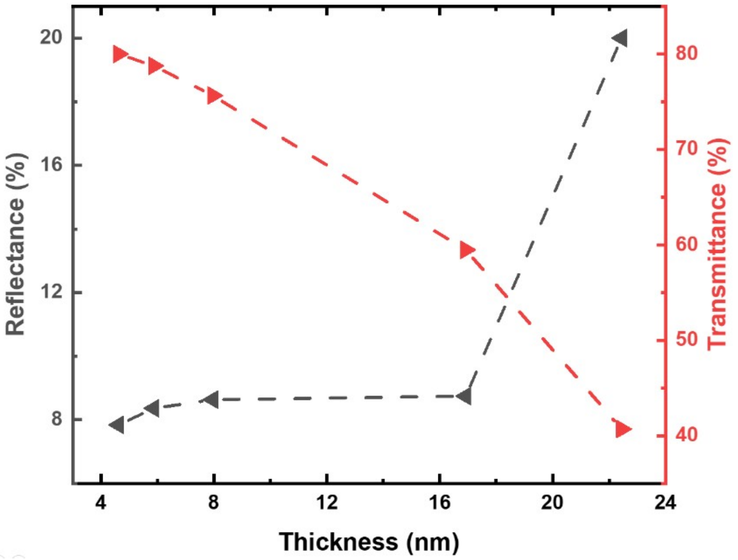

Figure S3. The experimentally measured transmittance and reflectance.

Table S1. The calculated values for the real and imaginary parts of the refractive index, as well as the absorption coefficient, are as follows.

Thickness (nm)	Layer	n	k	α*10⁴ (cm⁻¹)
22.44	34	3.434	0.778	12.21
16.92	27	2.667	0.717	11.26
7.96	13	2.929	0.556	8.73
5.87	9	2.958	0.543	8.52

4.62	7	3.343	0.414	6.50

S3. N_0^2/N_t^2-1 vs. t

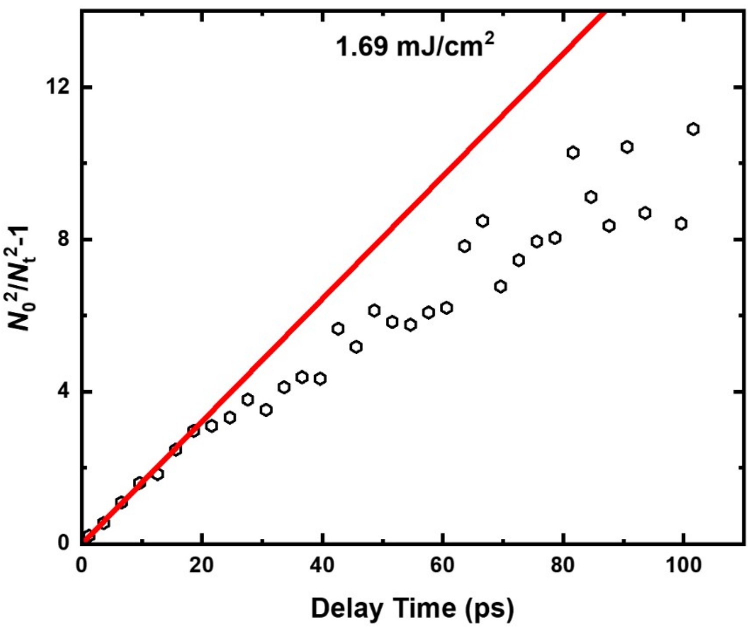

Figure S4. Plot of the relationship between N_0^2/N_t^2-1 and t at a thickness of 4.62 nm and a pump fluence of 1.69 mJ/cm^2. The red line represents the linear fit within the first 15 ps.

At a pump fluence of 1.69 mJ/cm^2, the 4.62 nm sample exhibits linear behavior for the first 15 ps, but becomes nonlinear after that time (> ~15 ps). This indicates that Auger recombination dominates at the first 15 ps.

S4. Sample uniformity

We checked the AFM data and obtained the height fluctuation of the surface, as shown in Figure S5(a). The fluctuation is no more than 5 Å. In addition, when we carried out the pump-probe experiment, three different test points were selected on every sample to check the repeatability, as shown in Figure S5(b). The results show that the electronic signals of the three sample points have good repeatability, and fitted decay time of the three spots are 129.56 ± 0.75 ps, 129.38 ± 0.74 ps, and 130.22 ± 0.87 ps, respectively, agreeing well within error bar range.

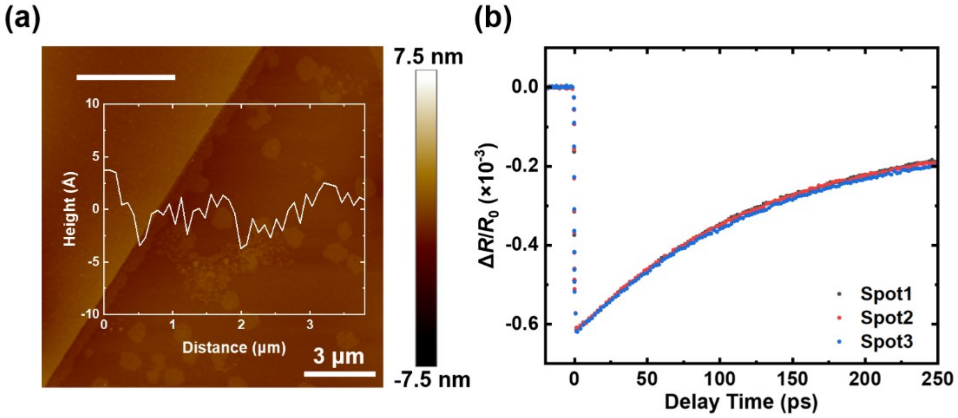

Figure S5. (a) The roughness of the sample surface. (b)Transient reflectivity curves of three sample points for 22.44 nm sample at a pump fluence of 3.03 μJ/cm^2. The black, red and blue dots represent the replacement of three different sample points for samples of the same thickness.

Reference:

1. G. Jnawali, D. Boschetto, L. M. Malard, T. F. Heinz, G. Sciaini, F. Thiemann, T. Payer, L. Kremeyer, F.-J. Meyer zu Heringdorf and M. Horn-von Hoegen, *Appl. Phys. Lett.*, 2021, **119**.